

MODELING AND CONTROL OF AN ELECTRIC POWER STEERING SYSTEM USING MODEL REFERENCE ADAPTIVE CONTROLLER

MÔ HÌNH HOÁ VÀ ĐIỀU KHIỂN HỆ THỐNG LÁI TRỢ LỰC ĐIỆN SỬ DỤNG BỘ ĐIỀU KHIỂN THÍCH NGHI DỰA TRÊN MÔ HÌNH

Le Hoai Nam, Pham Anh-Duc*

The University of Danang - University of Science and Technology, Vietnam

*Corresponding author: ducpham@dut.udn.vn

(Received: February 05, 2025; Revised: April 26, 2025; Accepted: May 06, 2025)

DOI: 10.31130/ud-jst.2025.039E

Abstract - Power-assisted steering systems (or power steering systems) are widely used in vehicles nowadays. Thus, evaluating the stability and accuracy of the control system for the power-assisted steering process is necessary. The paper presents the modeling and control of an electric power steering (EPS) system. The EPS plant model consists of three parts: motor, drive tires, and steering linkage, derived from basic electrical physics laws, virtual power principle, and TMeasy method, respectively. The model Reference Adaptive Control (MRAC) algorithm is chosen to deal with uncertainties in the system. These are implemented and simulated in MATLAB/ Simulink. The simulation result proved the proposed method's robustness and effectiveness, especially regarding disturbance resistance.

Key words - Tire Model easy to use (TMeasy); Model Reference Adaptive Control; Electric Power Steering (EPS) system.

1. Introduction

Power-assisted steering systems are widely used in vehicles nowadays. The common power steering systems can be classified into hydraulic power steering (HPS), electro-hydraulic power steering (EHPS), and electric power steering (EPS). Compared to traditional HPS, EPS offers several advantages such as energy efficiency, safety, adjustability of steering feel, modularity, and environmental friendliness. In particular, the increasing adoption of EPS in electric and hybrid vehicles has significantly contributed to the system's growing market share, which is projected to reach USD 39.5 billion by 2032 [1], [2].

However, unpredictable road conditions, frictional variations, and dynamic interactions between tires and road surfaces introduce considerable modeling and control challenges for EPS systems. Previous studies have employed various modeling strategies, such as data-driven lookup tables and single-track vehicle models. The former approach [3], [4] often suffers from high computational costs, while the latter [5] - [7] simplifies dynamic interactions, especially those related to road reaction torque and self-aligning torque, into an aggregated disturbance force.

To improve modeling fidelity without compromising computational efficiency, this study adopts the TMeasy tire model—an established semi-empirical method capable of capturing nonlinear tire behavior such as lateral slip, force

Tóm tắt - Hệ thống trợ lực đánh lái được ứng dụng rộng rãi trong xe hơi ngày nay. Do đó, việc đánh giá tính ổn định và sự chính xác hệ thống điều khiển quá trình trợ lực đánh lái của xe hơi là cần thiết. Bài báo trình bày việc mô hình hoá và điều khiển hệ thống lái trợ lực điện (EPS). Mô hình hệ thống lái trợ lực điện bao gồm ba phần là động cơ, lốp dẫn động, cơ cấu lái được lấy lần lượt từ các định luật vật lý cơ bản, nguyên lý công suất ảo và phương pháp TMeasy. Thuật toán điều khiển thích nghi dựa trên mô hình được lựa chọn để đối phó với các yếu tố bất định trong hệ thống. Việc này được thực hiện và mô phỏng trong MATLAB/Simulink. Kết quả mô phỏng đã chứng minh tính ổn định và hiệu quả của phương pháp đề xuất, đặc biệt là về khả năng chống nhiễu.

Từ khóa - Mô hình lốp TMeasy; Bộ điều khiển thích nghi dựa trên mô hình (MRAC); Hệ thống lái trợ lực điện.

saturation, and relaxation dynamics [8], [9]. TMeasy has also been validated in recent works concerning tire wear and vehicle response, demonstrating its suitability for real-time simulations [10], [11].

On the control side, the EPS system's inherent nonlinearities and uncertainties necessitate robust and adaptive control methods. Among these, Model Reference Adaptive Control (MRAC) has shown promising results in handling parameter variations and unknown disturbances [12], [13]. MRAC does not require a precise model of the plant and has been successfully applied to various automotive systems to enhance stability and responsiveness under real-world conditions.

In this paper, we present a comprehensive modeling and control framework for an EPS system using the TMeasy tire model and MRAC algorithm. The EPS plant includes three major components: the assist motor, the mechanical linkage, and the tire-road interaction. The MRAC controller is designed to adaptively regulate steering torque while compensating for modeling uncertainties and external disturbances. Simulations in MATLAB/Simulink are used to validate the proposed system under realistic operating conditions.

Compared to previous works that often address either simplified modeling [5], [6] or focus solely on control aspects [12] - [14], this research integrates a semi-physical tire model and an adaptive controller within a full EPS architecture. To the best of the authors' knowledge, such

an integrated approach-featuring both TMeasy-based tire modeling and MRAC for full EPS dynamics-has not been comprehensively investigated in the literature.

2. System general structure

EPS system includes three basic components: The Electric Control Unit (ECU), an assist motor, and a mechanical part consisting of mechanisms between the steering wheel and the tires. Its basic operating principle can be described as follows: when the steering tires are displaced, a self-aligning torque which tends to return the wheels to their original position, arises. This torque requires considerable steering effort to steer the vehicle, particularly at low speeds. The EPS system employs an electric motor to assist the driver in turning the steering wheel under such driving conditions. The role of the ECU is to determine the PWM control signal (Pulse Width Modulation) in order to provide a comfortable steering experience.

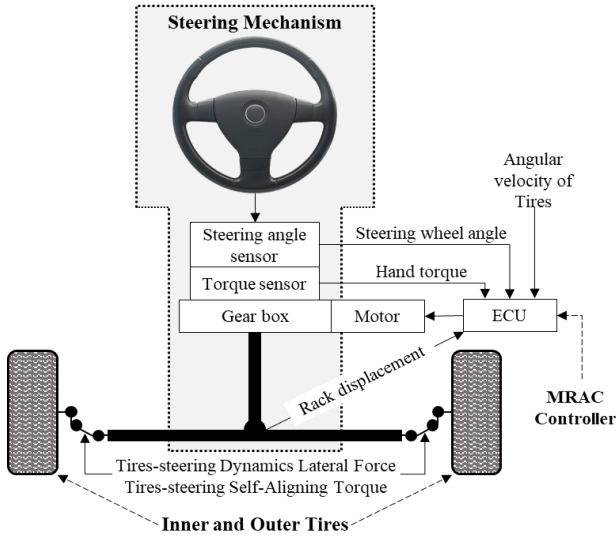


Figure 1. Electric Power Steering: System architecture

3. Plan model

3.1. One Tire model

The tire model block diagram is shown in Figure 2. Block “1” describes the kinematics while the remaining blocks, including equations derived in [8] represent the dynamics of steering tires. These blocks will be described in detail as follows.

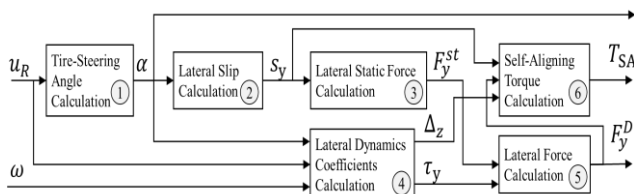


Figure 2. Block diagram of One Tire Model

In which:

- u_R : Rack displacement [m];
- α : Steering angle of steering tire [rad];
- s_y : Lateral slip of steering tire;
- F_y^{st} : Static lateral force of steering tire [N];

- T_{SA} : Self-aligning torque of steering tire [M];
- F_y^D : Dynamic lateral force of steering tire [N];
- Δ_z : Vertical tire deflection [m];
- τ_y : Time constant of 1st order tire dynamics equation;
- ω : Angle velocity of steering tire [rad/s].

3.1.1. Tire-steering angle calculation

The relationship between the slip angle and the rack displacement is derived based on Ackermann steering geometry as illustrated in Figure 3.

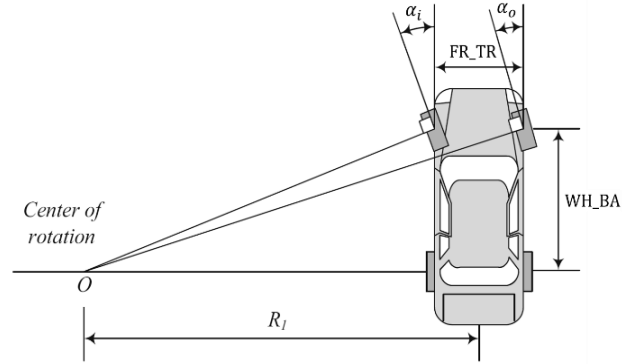


Figure 3. Ackermann steering geometry [11]

Table 1. Description of symbols in Figure 3

Symbols	Description	Unit	Value
α_o/α_i	Angle of outer/inter-steering tire	-	-
FR_TR	Front track of the vehicle	m	1.47
WH_BA	Wheel base of the vehicle	m	2.55

$$\alpha_o = \arctan \left(\frac{WH_BA \times \tan(i_{SL} u_R)}{WH_BA + \frac{1}{2} \times FR_TR \times \tan(i_{SL} u_R)} \right) \quad (1)$$

$$\alpha_i = \arctan \left(\frac{WH_BA \times \tan(i_{SL} u_R)}{WH_BA - \frac{1}{2} \times FR_TR \times \tan(i_{SL} u_R)} \right) \quad (2)$$

Table 2. Description of parameters in (1) and (2)

Parameters	Description	Unit	Value
i_{SL}	Constant ratio of steering linkage	-	9.3

3.1.2. Lateral slip calculation

$$s_y = \tan \alpha \quad (3)$$

3.1.3. Lateral static force calculation

The static lateral force F_y^{st} can be determined as follows:

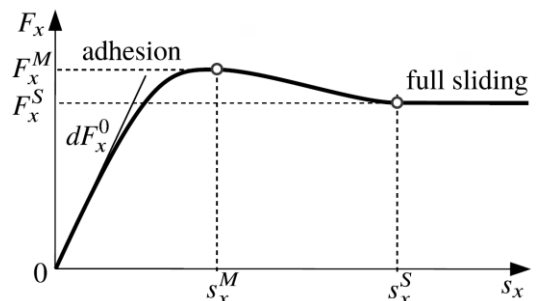


Figure 4. Typical longitudinal force characteristic [7]

Table 3. Description of symbols in Figure 4

Symbol	Description	Unit	Value
dF_y^0	Init slope in the lateral direction	-	66000
F_y^M	Maximum lateral force	N	2950
F_y^S	Lateral force in full sliding state	N	2800
s_y^M	Lateral slip where $F_y = F_y^M$	-	0.205
s_y^S	Lateral slip where $F_y = F_y^S$	-	0.5

3.1.4. Lateral dynamics coefficients calculation

a. Tire deflection Δ_z

$$\Delta_z = r_0 - r_s = \frac{-\sqrt{2c_{z1}^2 - c_{z2}^2} + \sqrt{|2c_{z1}^2 - c_{z2}^2| + c_{z2}^2 - c_{z1}^2}}{\frac{c_{z2}^2 - c_{z1}^2}{2F_z^N}} \quad (4)$$

Table 4. Description of parameters in equation (4)

Parameters	Description	Unit	Value
c_{z1}	Radial stiffness at nominal load	N/mm	190
c_{z2}	Radial stiffness at double payload	N/mm	206
F_z^N	Gravity load (nominal load) of the car	N	3200
r_0	Unloaded tire radius	m	0.3085
r_s	Deflected or static tire radius	m	-

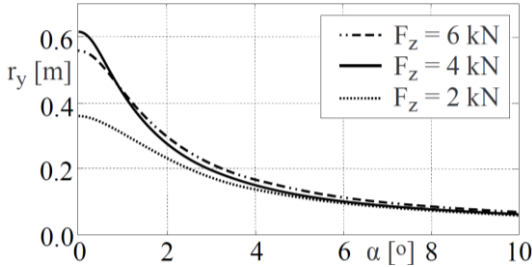
b. Time constants τ_y

$$\tau_y = \frac{r_y}{r_D |\omega|} \quad (5)$$

Dynamic rolling radius r_D :

$$r_D = \frac{2}{3}r_0 + \frac{1}{3}r_s \quad (6)$$

Relaxation length r_y is a function of the static vertical force F_z^{st} and the slip angle α_s and can be determined from experimental data, as shown in Figure 5.

**Figure 5.** Measured lateral force relaxation length for a typical passenger car tire [8]

The wheel load (vertical force F_z^{st}) is calculated as follows:

$$F_z^{st} = \sqrt{2c_{z1}^2 - c_{z2}^2} \times \Delta_z + \frac{c_{z2}^2 - c_{z1}^2}{4F_z^N} \times (\Delta_z)^2 \quad (7)$$

3.1.5. Lateral force calculation

$$F_y^D(s) = \frac{1}{\tau_y \times s + 1} F_z^{st}(s) \quad (8)$$

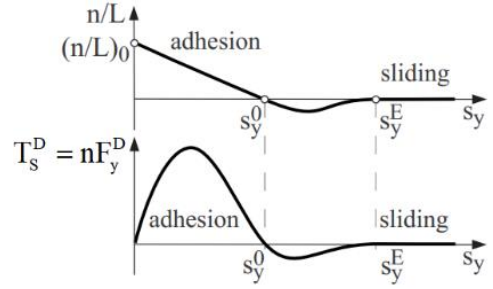
(s in this equation is Laplace variable)

3.1.6. Self-aligning torque calculation

The dynamic self-aligning torque of the tire can be approximated using the following expression:

$$T_z = T_s^D = -nF_y^D \quad (9)$$

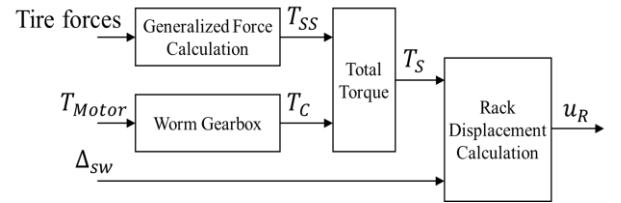
Here, n denotes the steady-state tire offset and can be calculated as a function of s_y , as illustrated in Figure 6.

**Figure 6.** Typical plot of lateral force, normalized tire offset, and self-aligning torque [8]**Table 5.** Description of symbols in Figure 6

Symbol	Description	Unit	Value
$(n/L)_0$	Normalized caster offset n/L when $s_y = 0$	-	0.178
s_y^0	s_y where n/L passes s_y axis	-	0.2
s_y^E	s_y where n/L approaches s_y axis again	-	0.35

3.2. Rack-and-pinion steering mechanism

The steering mechanism model block diagram is shown in Figure 7. The model takes the tire forces, the torque provided by the assist motor, and the wheel steering angle as its inputs, and outputs the rack displacement.

**Figure 7.** Block diagram of the steering mechanism

In which:

- $T_{\text{tire forces}}$: Lateral forces and self-aligning torques introduced in the previous part [N, M]
- T_{Motor} : Torque provided by motor [M]
- T_{SS} : Generalized force applying to steering shaft [M]
- T_C : Output torque of worm gearbox [M]
- T_S : Total torque applying to steering shaft [M]

3.2.1. Generalized force calculation

$$T_{SS} = c \times (\text{abs}(F_{yi}^D) + \text{abs}(F_{yo}^D) + \text{abs}(T_{SAi}) + \text{abs}(T_{SAo})) \quad (10)$$

In which:

- $F_{yi/0}^D$: Lateral dynamic forces of inner/outer tire [N];
- $T_{SAi/0}$: Self-aligning torque of inner/outer tire [M].

Table 6. Description of parameter in equation (10)

Parameters	Description	Unit	Value
c	Caster offset	m	0.030326

3.2.2. Worm gear box

$$T_C = k_{WG} \times T_{\text{Motor}} \quad (11)$$

Table 7. Description of parameter in equation (11)

Parameters	Description	Unit	Value
k_{WG}	Constant efficiency of worm gearbox	-	0.92

3.2.3. Total torque calculation

$$T_S = T_h + T_C - \frac{T_{SS}}{i_S} \quad (12)$$

Table 8. Description of parameter in equation (12)

Parameters	Description	Unit	Value
i_s	Overall ratio of the steering wheel to steering tire	-	13.5

3.2.4. Rack displacement calculation

$$u_R = \frac{1}{i_{SB}} \left(\Delta_{SW} - \frac{T_S}{c_S} \right) \quad (13)$$

Table 9. Description of symbols in equation (13)

Parameters	Description	Unit	Value
i_{SB}	Ratio of the steering box	rad/m	125

3.3. Electric motor

The electric motor can be represented by transfer function as described in [10]:

$$T_c(s) = G_{T_c}(s) \times V_a(s) = \frac{i_m \times J \times K_m \times s \times V_a(s)}{J \times L_a \times s^2 + (J \times R_a + B \times L_a) \times s + (R_a \times B + K_m \times K_b)} \quad (14)$$

In which:

- e_a : Voltage applied to the motor's armature [V];
- i_a : Current appear in armature circuit [A];
- e_b : The back electromotive force [V];
- R_f : Field part's electric resistance [Ω];
- L_f : Field part's electric inductance [H];
- i_f : Current appear in field circuit [A];
- $T_{Motor}(s)$: Torque created by motor [Nm];
- $\omega(s)$: Angular velocity of motor [rad/s];
- s : Laplace variable.

Table 10. Motor parameters

Parameters	Description	Unit	Value
R_a	The armature part's electric resistance	Ω	0.086
L_a	The armature part's electric inductance	H	0.00163
J	Inertia load	kg/m^2	125
B	Friction constant of the motor	Nm.s/rad	5.05×10^{-6}
K_m	Motor torque constant	Nm/A	53.6×10^{-3}

4. Proposed control algorithm: Model Reference Adaptive Control for SISO system

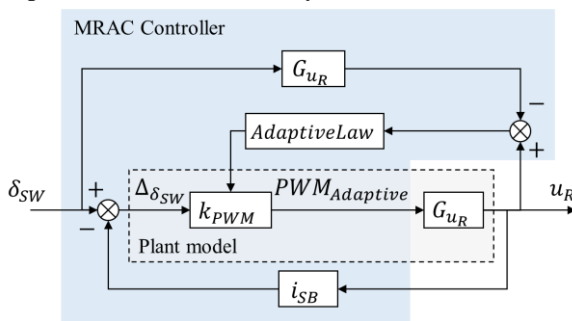


Figure 8. System architecture with MRAC algorithm

4.1.1. Single input single output (SISO) plant model

Considering T_h and T_{SS} as uncertainties, the model of the EPS plant can be described as shown in Figure 9.

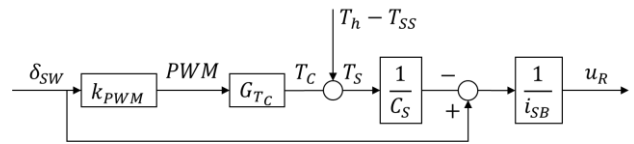


Figure 9. Block diagram of SISO EPS system

Let $a_{u_r} = 1 - \frac{T_h - T_{SS}}{C_S}$, $b_{u_r} = \frac{k_{PWM}}{C_S}$, the transfer function of the EPS plant system can be achieved by applying block diagram reduction as follows:

$$G_{\text{Plant}}(s) = \frac{u_R(s)}{\delta_{SW}(s)} = \frac{0.204a_{u_R}s^2 + (10.75a_{u_R} - 171b_{u_R})s + 0.003a_{u_R}}{25.4625s^2 + 1343.75s + 0.37} \quad (15)$$

4.1.2. Reference model

The reference model is selected based on “Step response of EPAS system to driver torque” as described in [13].

To enhance the performance of the control algorithm, the overshoot component is eliminated and the rise time is reduced to 0.01s. Let A_{Ref} , B_{Ref} be the denominator and the numerator of the transfer function of the reference model; thus, its transfer function can be written as follows:

$$G_{\text{ref}} = \frac{u_R}{\delta_{SW}} = \frac{B_{\text{ref}}}{A_{\text{ref}}} = i_{SB} \frac{1}{0.01s + 1} \quad (16)$$

4.1.3. Adaptive law

Let A_{plant} , B_{plant} denote the denominator and numerator of the transfer function of the plant. By applying block diagram reduction, we obtain:

$$\frac{u_R}{\delta_{SW}} = \frac{\frac{B_{\text{Plant}}}{A_{\text{Plant}}}}{1 + i_{SB} \times \frac{B_{\text{Plant}}}{A_{\text{Plant}}}} = \frac{B_{\text{Plant}}}{A_{\text{Plant}} + i_{SB} \times B_{\text{Plant}}} \quad (17)$$

Adaptive law:

$$\frac{d(k_{\text{PWM}})}{dt} = \frac{\gamma}{i_{SB}} \times \Delta_{u_R} \times \Delta_{\delta_{SW}} \times \frac{1}{0.01s + 2} \quad (18)$$

$$\text{PWM}_{Adaptive} = \text{PWM}_0 + k_{\text{PWM}} \quad (19)$$

In which:

- $PWM_{Adaptive}$: Output of adaptive process. Input signal of motor.

Table 11. Description of symbols in equations (18) and (19)

Symbols	Description	Unit	Value
γ	Adaptive coefficient, determined using Model-In-the-Loops method	-	0.1
PWM ₀	Initial PWM signal, determined using Model-In-the-Loops method	-	0.4

5. Simulation results and discussion

5.1. Simulation environment

The system is built and simulated in the MATLAB/Simulink development environment. There are two scenarios considered under normal driving situations with the vehicle traveling at approximately 80 km/h and representing two typical driver behaviors.

5.2. Simulation results

5.2.1. Scenario 1

The input signal of the system which is the steering wheel signal is in the form of a sinusoid.

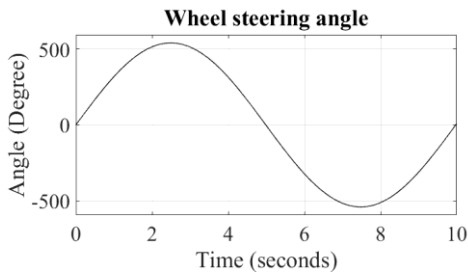


Figure 10. Input of test scenario 1

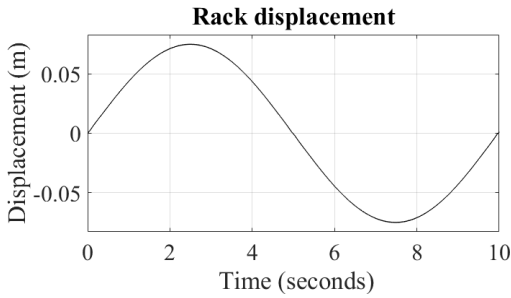


Figure 11. Output of EPS system: Rack displacement

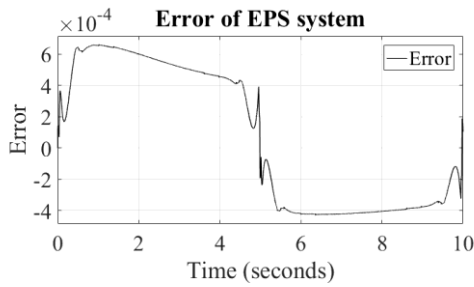


Figure 12. Error of EPS system

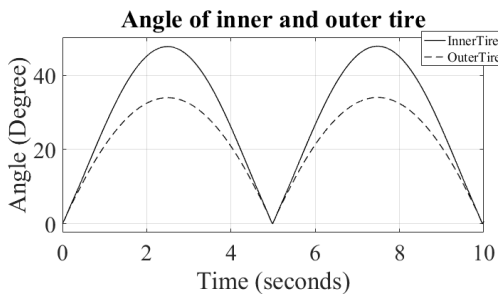


Figure 13. Output of EPS system: Inner/Outer tire angle

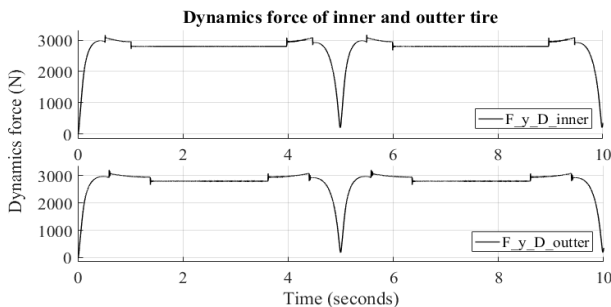


Figure 14. Output of EPS system: Dynamics force of Inter/Outer tire

5.2.2. Scenario 2

The input signal of the system is in the form of step response of first order system as follows:

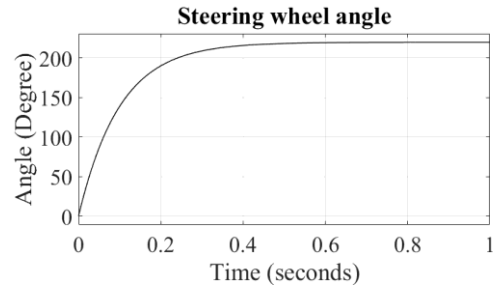


Figure 15. Input of test scenario 2

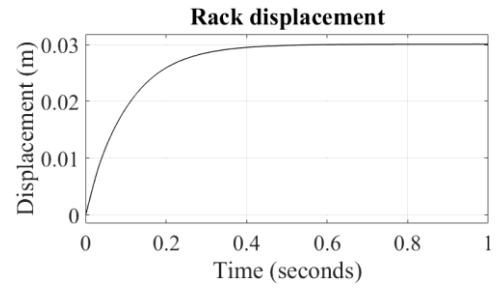


Figure 16. Output of EPS system: Rack displacement

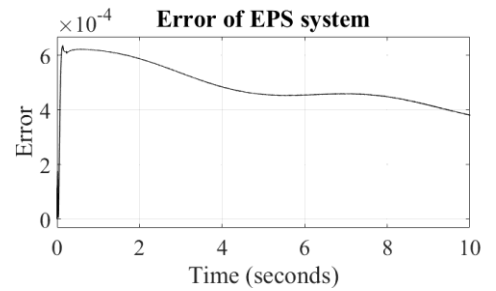


Figure 17. Error of EPS system

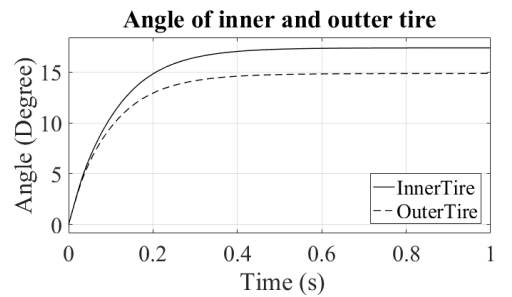


Figure 18. Output of EPS system: Inner/Outer tire angle

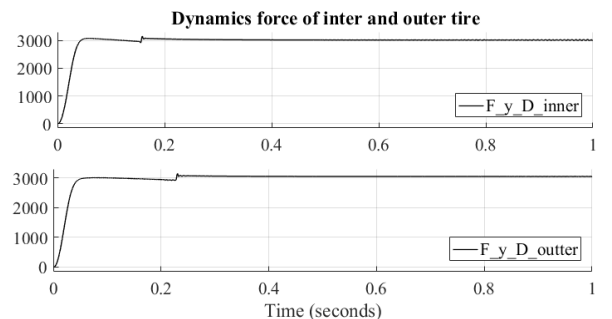


Figure 19. The output of EPS system: dynamics force of Inter/Outer tire

5.3. Discussion

The simulation results above demonstrate the response of the EPS system with the MRAC controller under normal driving conditions. The control error of MRAC-based EPS system was relatively low (as shown in Figures 12 and Figure 17) and tend to decrease as time increases because of the adaptive process.

In the steady-state case, even under perturbations, the MRAC controller maintained good performance and robustness. However, in situations involving relatively high vehicle acceleration, accurate modeling became challenging due to increased sensitivity to noise, which led to the formulation of a new differential equation. The problem of modeling EPS dynamics under high acceleration conditions remains an open research question.

In addition, the column-type Ackermann geometry was introduced and modeled. Simulation results showed that the steering angle of the inner tire was consistently greater than that of the outer tire, consistent with Ackermann geometry. This design helps ensure driving safety and prolongs the lifespan of the steering tires.

From a system dynamics perspective, the EPS model performed well overall, as the simulated tire steering forces exhibited a similar pattern to the reference data presented in [4]. However, some irregularities were observed, which can be attributed to tire deflection phenomena and the use of simplified approximating functions for the relationships described in Section 3.

6. Conclusion

This paper presented the development of a plant model for an Electric Power Steering (EPS) system, which effectively captures the system's nonlinearities and uncertainties under real-world conditions. The column-type Ackermann steering geometry was introduced and modeled. Additionally, the TMeasy modeling method was employed to represent the tire deflection phenomenon using the side-slip domain instead of the traditional time or frequency domains. An MRAC algorithm was also proposed, implemented, and analyzed.

The influence of vehicle acceleration and the application of alternative control strategies-such as input-output linearization and sliding mode control-will be investigated in future work.

Acknowledgment: This research was supported by engineers Nguyen Ba Thang and Ngo Hoang Trung during the modeling and testing of the system.

REFERENCES

- [1] GlobeNewswire, "Electric Power Steering Market Size to Reach USD 39.50 Billion", *GlobeNewswire*, 2024. [Online]. Available: <https://www.globenewswire.com/news-release/2024/09/27/2954418/0/en/Electric-Power-Steering-Market.html>. [Accessed: Jan. 15, 2025].
- [2] Grand View Research, "Electric Power Steering Market Size & Share Report, 2030", *Grand View Research*, 2024. [Online]. Available: <https://www.grandviewresearch.com/industry-analysis/electric-power-steering-market-report>. [Accessed: Jan. 15, 2025].
- [3] X. Chen, T. Yang, X. Chen, and K. Zhou, "A generic model-based advanced control of electric power-assisted steering systems", *IEEE Transactions on Control Systems Technology*, vol. 16, no. 6, pp. 1289–1300, Jun. 2008.
- [4] J.-H. Kim and J.-B. Song, "Control logic for an electric power steering system using assist motor", *Mechatronics*, vol. 12, no. 4, pp. 447–459, Apr. 2002.
- [5] D. Saifia, M. Chadli, H. R. Karimi, and S. Labiod, "Fuzzy control for electric power steering system with assist motor current input constraints", *Journal of the Franklin Institute*, vol. 352, no. 2, pp. 562–576, Feb. 2015.
- [6] M. Chatterjee, C. Rajguru, and A. Wadkar, "Mathematical modelling of automotive electric power assist steering system", in *2013 International Conference on Advances in Computing, Communications and Informatics (ICACCI)*, Aug. 2013.
- [7] X. Li, X.-P. Zhao, and J. Chen, "Controller design for electric power steering system using T-S fuzzy model approach", *International Journal of Automation and Computing*, vol. 6, no. 2, pp. 198–203, May 2009.
- [8] G. Rill and A. Arrieta Castro, *Road Vehicle Dynamics: Fundamentals and Modeling with MATLAB*, 2nd ed. Boca Raton, FL, USA: CRC Press, 2020.
- [9] A. Mas, "Tire wear modelling, simulation and validation with measurements", *MSc Thesis*, Universitat Politècnica de Catalunya, 2024.
- [10] R. C. Dorf and R. H. Bishop, *Modern Control Systems*, 12th ed. Upper Saddle River, NJ, USA: Pearson, Jan. 2016.
- [11] R. N. Jazar, *Vehicle Dynamics: Theory and Application*. New York, NY, USA: Springer, May 2017.
- [12] Y. Li, R. Zhou, Q. Zheng, and L. Yang, "Design of model reference adaptive control law of steering mechanism for heavy duty vehicle", in *IEEE 10th International Conference on Industrial Informatics*, Jul. 2012.
- [13] M. Parmar and J. Y. Hung, "A sensorless optimal control system for an automotive electric power assist steering system", *IEEE Transactions on Industrial Electronics*, vol. 51, no. 2, pp. 290–298, Apr. 2004.
- [14] N. D. M. Phan, N. Q. H. Tran, H. C. Nguyen, and T. Hoang, "Design and Evaluate Controller for Power Steering System", *The University of Danang - Journal of Science and Technology*, vol. 21, no. 11.2, pp. 31–35, 2023. [Online]. Available: <https://jst-ud.vn/jst-ud/article/view/8822/6054>